Raja Yahmadi[2], Kais Brik[1,*], Faouzi Ben Ammar[2],

J. Electrical Systems 20-4 (2024): 415-432

Regular paper

A new methodology of battery lifetime estimation related to the depth of discharge in the standalone photovoltaic applications

The operating conditions of the battery storage in the standalone photovoltaic (PV) application have an important influence on its electrical and physicochemical properties. Consequently, it is important to elaborate a mathematical aging model in order to estimate the battery lifetime and to determine their replacement time. In this context, this paper presents a new methodology lifetime estimation of battery storage under operating conditions related to the depth of discharge. The proposed methodology is based firstly on the modeling of the battery by an electrical equivalent circuit. Then, the research of the correlation between the electrical equivalent circuit parameters and the various degradation modes is carried out. An analysis of the voltage drops by the variation of the electrical parameters is done to develop the mathematical expressions that adequately describe the rated capacity loss of the battery according to each degradation mode. This study is completed by the use of these capacity losses to develop a diagnostic system allowing the estimation of the number of battery remaining cycles taking into account the depth of discharge. Therefore, this new methodology allows drawing conclusions about the battery lifetime and its available rated capacity in the standalone photovoltaic application.

Keywords: Battery; Electrical equivalent circuit; Depth of discharge; Aging; Available capacity; Lifetime.

1. Introduction

The use of the electrical energy storage system is a primordial solution to optimize energy resources in the various power electronic applications. The development of energy storage systems can be considered as the heart of the standalone photovoltaic system that allows compensating the intermittent and the fluctuation of the renewable energy sources [1-5].In these applications, the lead acid batteries are widely applied due to their low-costs, high rate of recycling, ease manufacturing process and availability in large quantities [6]. One main limitation of these technologies resides in the battery ageing.

During the exploitation phase, a shutdown of the lead acid battery due to the unfavorable conditions in the PV applications causes a major problem [7-9]. The principal signatures of the end of battery lifetime are related to the dramatic acceleration of aging mechanisms. These aging mechanisms are the stratification of the electrolyte, the corrosion of the electrodes, the hard sulfating phenomenon and the poor-cohesion of active mass [10,11]. Indeed, the impact of these aging mechanisms on the battery performances results in an increase of the rated capacity loss.

With the rise of the energy storage element use, it is necessary to incorporate a battery lifetime estimation model. In fact, the estimation of the lifetime indicators is challenging and remains an area of active research. Recently, much diagnostic analysis has been

* Corresponding author: K. Brik, Research Laboratory of Materials, Measurements and Applications University of Carthage, Urban Center Nord BP 676-1080 Tunis Cedex. Tel(+216) 71 703 829. Fax (+216)71 704 329.E-mail address: kais.brik@yahoo.fr

[1]Higher Institute of Multimedia Arts of Manouba (ISAMM), University of Manouba, Tunis

[2]Institute of Applied Sciences and Technology, University of Carthage , Tunis

developed to indicate the lead acid battery lifetime such as electrochemical models, performance models, statistical approach and genetic algorithm [12-17]. The authors propose to develop methodology lifetime estimation for battery storage which takes into account the weaknesses of the different models. Indeed, the electrochemical model requires an important simulation time related to the complex numerical algorithms and requires also battery specific information that is difficult to obtain [18, 19].The performance model cannot properly model all the aging phenomena and requires a database about the battery specific information [20, 21]. Similarly, the statistical method requires a large amount of data to be reliable [21,22]. However, the genetic algorithms are time consuming calculation and its adjustment is delicate [23].

To address these issues related to the important simulation time and the necessity of a database in this work, the authors propose new methodology battery lifetime estimation. This methodology consists to elaborate a mathematical aging model based on the modeling of the battery by an electric equivalent circuit. Meanwhile, the proposed aging model estimates the number of battery remaining cycles during its operation period related to the depthof discharge. The methodology lifetime estimation of the lead acid battery contains three stages.

In the first stage, a topology description of the photovoltaic system is firstly presented.

The second stage consists of analyzing the degradation of the battery. Firstly, the battery is modeled by an electrical equivalent circuit that presents the Ohmic, charge transfer and diffusion phenomena. Then, the study of the correlation between the electrical equivalent circuit parameters and the different degradation modes is performed. The correlation study is completed by developing an approach that allows describing adequately the available rated capacity. This approach is based on the determination of the capacity loss associated with each degradation mode by simulation analysis of the parameter variation. The results obtained allows to develop a relationship that expresses the available rated capacity as a function of the various capacity losses associated with each degradation mode.

The third stage consists to propose a diagnostic system that allows estimating the number of the battery remaining cycles related to the depth of discharge. Finally, the proposed diagnostic system is applied to evaluate the lifetime of three used batteries. In this context, the identification of the electrical parameters of the batteries is carried out with experimental measurements of their voltage response.

2. Topology description of standalone photovoltaic system

The stand-alone photovoltaic system is a system that dependent only solar energy as a source of electrical energy. This system is composed of a DC–DC buck converter, PV generator, a bidirectional DC-DC converter and battery packs. The battery packs store the energy produced by PV generator during the day (sunshine phase) and serving during the night (dark phase) or during periods when solar radiation is insufficient. Fig. 1 shows the configuration of a standalone photovoltaic system with battery energy storage.

The DC–DC buck converter is controlled by a Maximum Power Point Tracking (MPPT) that presents oscillations around the Maximum Power Point (MPP) of the PV generator. In fact, the output voltage and output current of the PV generator are detected and sent to the MPPT controller. However, the bidirectional DC–DC converter provide the charging and discharging mode of the battery packs

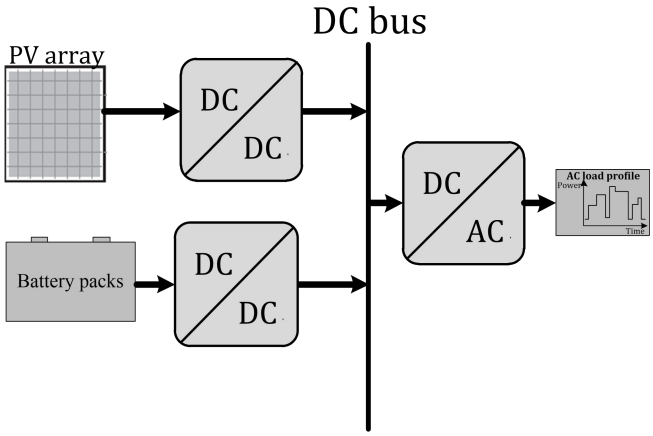

Fig 1.Configuration of the standalone photovoltaic system..

3. Degradation analysis of the battery

3.1. Modeling of the battery

The battery lifetime estimation is a complex process that cannot be directly measured from the battery. For that, a modeling of the battery by an electrical equivalent circuit is required. The electrical equivalent circuit parameters can be identified through the experimental measurements of the Standard impedance spectroscopy (EIS). The EIS is performed by exciting the battery with small sinusoidal currents to prevent a significant change of the State Of Charge (SOC) and for different frequency. Then, the response is recorded and plotted in Nyquist diagram.

In this section,an electrical equivalent circuit model of the battery based on the results of impedance spectroscopy is introduced. This study starts with an experimental measurement carried out on a new flooded lead acid battery with a rated capacity given by the manufacturer ($C_{manufactured}$) of 90 Ah and a rated voltage of 12V. The Nyquist diagram is performed with small sinusoidal currents Idc = 100 mA at SOC = 100%, the amplitude of the AC perturbation 10mV, and a frequency range [10 mHz- 500 Hz].

Figure 2 illustrates the simplified electrical equivalent circuit with the corresponding effects in the Nyquistdiagram of the new flooded lead acid battery.The Nyquistdagram (Figure 2.a) allows to graphically visualizing three respective influence zones: Ohmic zone, the charge transfer zone and the diffusion zone. By the mean of Nyquist diagram, a simplified electrical equivalent circuit is developed as shown in figure 1.b[24, 25].

With :

E_{eq}: Equilibrium potential,

R_{Ω}: Internal resistance,

R_{tc}: Charge transfer resistance,

C_{dl}: Double layer capacity,

Z_{ω} : Diffusion impedance.

The diffusion impedance presents an infinite sum of parallel RC cells and can be express by equation (1).

$$Z_\omega(t) = \frac{1}{C_\omega}\exp\left(-\frac{t}{R_{\omega 1}C_\omega}\right) + \frac{1}{C_\omega}exp\left(-\frac{t}{R_{\omega 2}C_\omega}\right) + \ldots + \frac{1}{C_\omega}exp\left(-\frac{t}{R_{\omega k}C_\omega}\right) \quad (1)$$

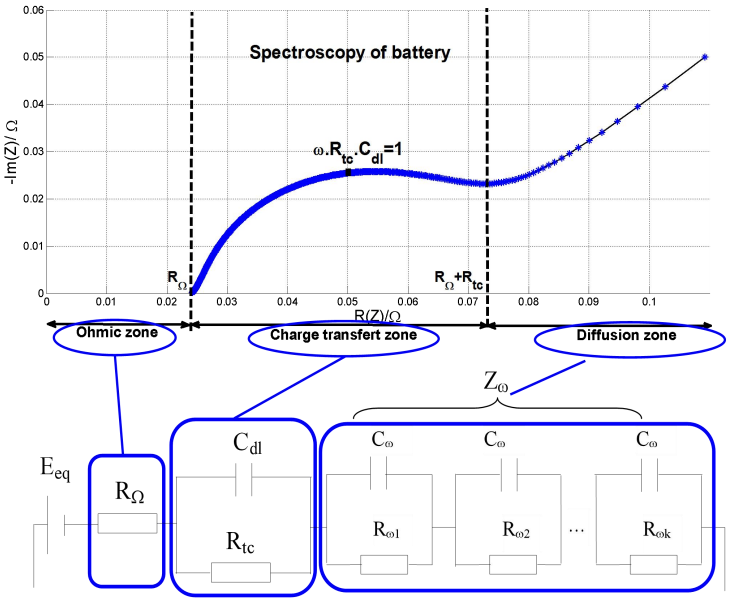

Fig. 2.a:Nyquist diagram of battery, b:Electrical equivalent circuit.

The expression of the constants is given by the following equations (2):

$$C_\omega = \frac{K_1}{2K_2^2},\ R_{\omega,k} = \frac{8K_1}{(2k-1)^2\pi^2},\ with\ \sum_{k=1}^{k=\infty}\frac{1}{(2k-1)^2} = \frac{\pi^2}{8} \quad (2)$$

From the Nyquist diagram of the battery (Figure 2,a), the parameters R_Ω, R_{tc}, and C_{dl} are determined graphically.The parameters K_1 and K_2 are identified by the least squares method by minimizing the criterion of the equation (3) for the performed N experimental measurements. This method allows to select among the functions U_{model_i}(i = 1 ... N) those which reproduce the best experimental data $U_{measure\_i}$.

$$S(K_1, K_2) = \sum_i^N \left[\frac{U_{measure\_i} - U_{model\_i}}{U_{measure\_i}}\right]^2 = \sum_i^N \varepsilon_i\,(t)^2 \quad (3)$$

The results of the identification are shown in Table 1.

Table 1: Estimated electrical equivalent circuit parameters of the new flooded battery.

	Value
E_{eq} (V)	12.84
R_Ω (Ω)	0.024
R_{tc}(Ω)	0.036
C_{dl} (F)	330
K_1	6.45 10^2
K_2	9.5610^{-3}

3.2. Correlation between the electrical equivalent circuit parameters and the various degradation modes

The lead acid batteries are storage means sensitive to the operating conditions [27,28]. Indeed, many factors such as cycling, overcharge, charge incomplete and deep discharge limit the battery performance by the appearance of different degradation modes, namely electrolyte stratification, hard sulfating of electrodes, corrosion of electrodes and poor-cohesion of the active mass. In fact, these various degradation modes change the properties of the battery and act on the electrical equivalent circuit parameters [26,29,30].

The approach presented in this paper for the mathematical ageing model development requires a study of the correlation between the degradation modes and the electrical parameters, which is the challenging goal [31]. The internal resistance R_Ω results the sum of connector resistances and electrolyte resistance. The variation of R_Ω causes an over voltage ΔV_{Ohmic} and shows the appearance of the electrolyte stratification and the electrodes corrosion. In fact, the corrosion of electrode appears when the electrolyte level is too low, the electrodes come into contact with the air and become oxidized. The lead Pb of the positive grid is converted to lead dioxide PbO_2 that leads to the increase in resistance across the corrosion layer between the grid and the active mass [32]. Consequently, the electrode corrosion increases the internal resistance R_Ω by the variation of the connector resistances in the positive and negative electrode.

However, the electrolyte stratification occurs due to the differences in the acid concentration, in which the acid is frequently denser at the bottom of the battery [33]. The electrolyte stratification increases the electrolyte resistance and therefore the internal resistance R_Ω is increased.

The poor-cohesion of the active mass generates on the electrode potential a second over voltage of charge transfer ΔV_{tc} and presents the variation of the charge transfer resistance R_{tc} and the double layer capacitance C_{dl} during the battery life cycles. The poor-cohesion of the active mass comes from the loss of active mass and shedding. The shedding show a mechanical loosening while the loss of active mass is related to loosening of the active mass particles that resulting in a loss of electronic conductivity[4].

The change in distribution of impedances (K_1 and K_2) generates on the electrode potential an over voltage $\Delta V_{diff}$and indicates the existence of the hard sulfating phenomenon. The hard sulfating phenomenon is occurring when the lead sulfate crystals ($PbSO_4$) are crystallized and cannot be removed during charging mode. This lead to the decrease of the active mass amount and so the diffusion of the acid is slow down [32].

Consequently, the aging of lead acid battery causes a decreasing of the available rated capacity and the battery will fully discharge faster than a new battery. The correlation between the degradation modes and the electrical equivalent circuit parameters is presented in Figure 3.

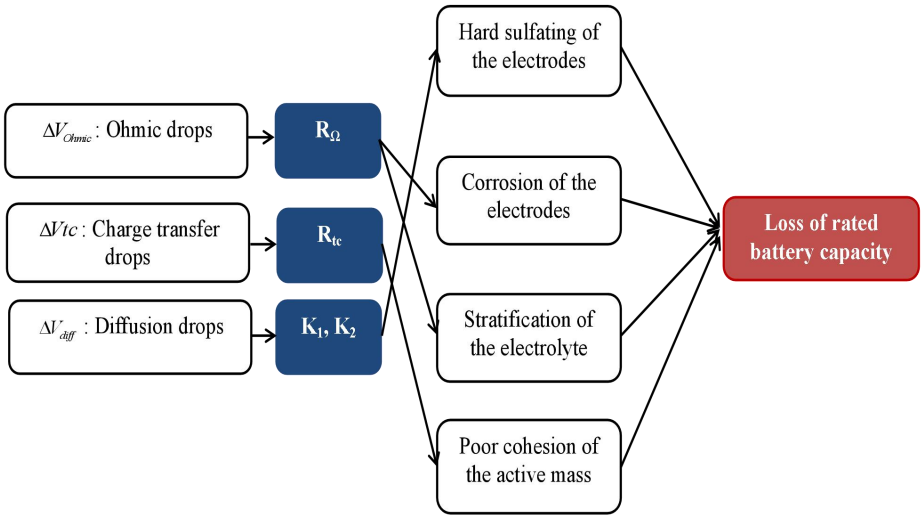

Fig. 3. Correlation between the degradation modes and the electrical equivalent circuit parameters

3.3. Analysis of available rated capacity

Several factors affecting the available rated capacity of the battery such as cycling, deep discharge, overheated, overcharge and charge incomplete. In fact, during the battery lifecycle, a repeated chemical transformation of the active mass is produced and creates changes in its morphology.

This change is shown by a modification in the cohesion, PbO_2 distribution and crystal size that generates a slow deterioration of the chemicals in the active mass. Consequently, the active mass volume is reduced and hence causes a decrease of the available rated capacity of the battery. For that, the authors propose an approach to determinate the available battery rated capacity by analysis the voltage drops.

In this section, the particular details of the proposed approach for analysis the available rated capacity is provided as depicted in Figure 4.This approach starts with a harmonic characterization of the fully charged battery. Then, the identification of the electrical equivalent circuit parameters from the Nyquist diagram is carried out (Section 2).

The identified parameters are used to simulate the voltage response of fully charged battery with discharge current $C_{manufactured}/10$.

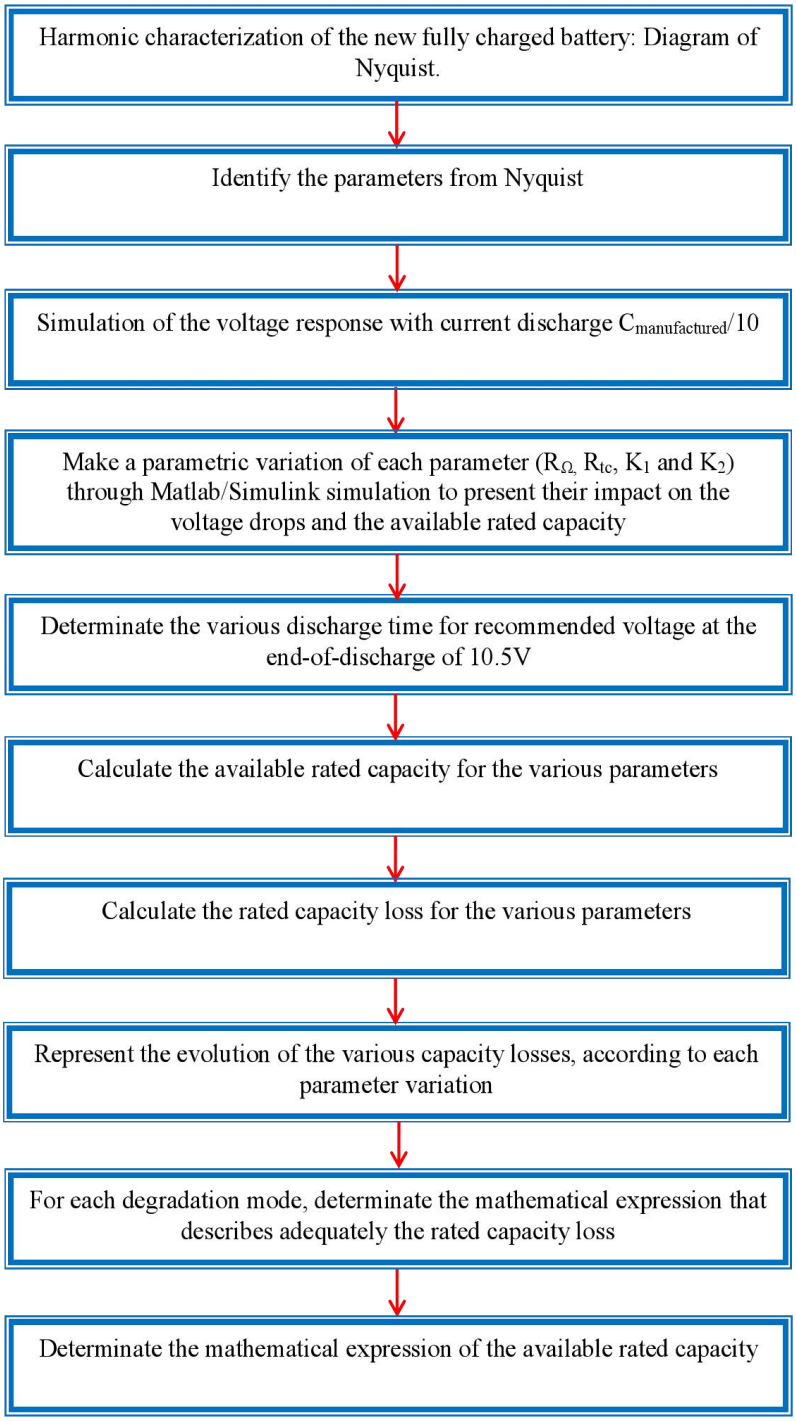

Fig. 4. Analysis approach of the available rated capacity

$$C_{arc} = \frac{I_{Cmax/10} * t_d}{3600} \quad (4)$$

With:

$I_{Cman/10}$: Discharge current

The rated capacity loss ΔC is determined by equation (5).

$$\Delta C = C_{man} - C_{arc} \quad (5)$$

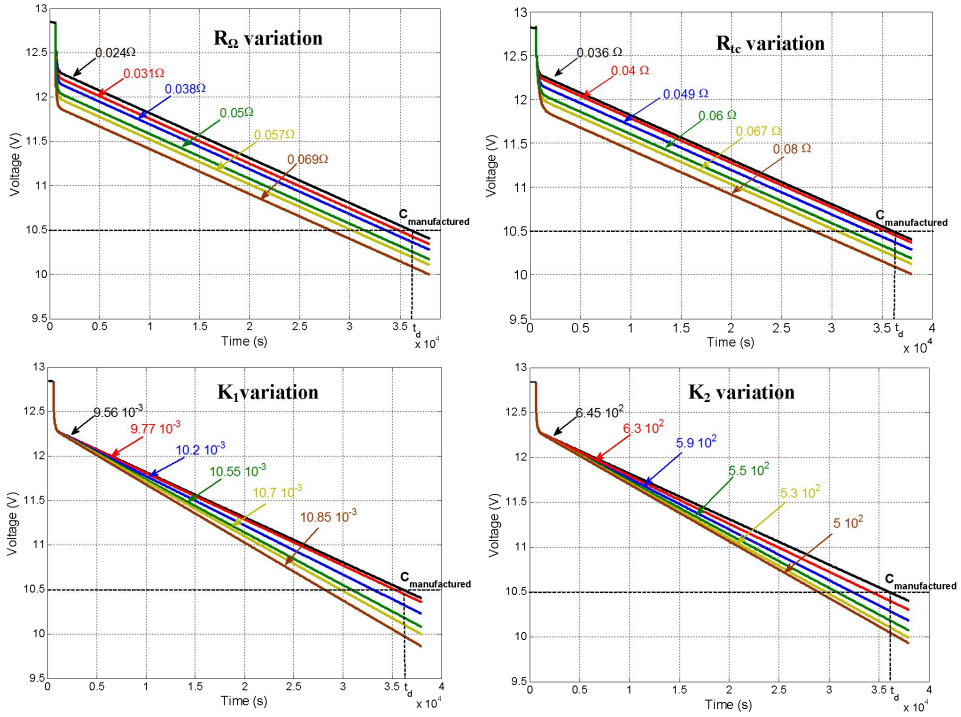

Fig. 5. Impact of the parameter variation on the battery voltage response during the discharge mode

From the identification of discharge time t_d, the available rated capacity and the capacity loss are determinate as illustrated in Table 2.

Table 2: Available rated capacity and capacity loss of the battery for each parameters variation

Parameters		t_d (s)	C_{arc} (Ah)	ΔC (Ah)
$R_Ω$	0.024	36000	90.00	0
	0.031	34815	87.04	2.96
	0.038	33568	83.92	6.08
	0.05	31431	78.57	11.43
	0.057	30185	75.46	14.54
	0.069	28051	70.12	19.88
R_{tc}	0.036	36000	90.00	0
	0.04	34815	88.37	1.63
	0.049	33746	84.36	5.64
	0.06	31788	79.47	10.53
	0.067	30541	76.35	13.65
	0.08	28228	70.57	19.43

K_1	6.45 102	36000	90.00	0
	6.3 102	35242	88.10	1.9
	5.9 102	33053	82.63	7.37
	5.5 102	30865	77.16	12.84
	5.3 102	29771	74.42	15.58
	5 102	28130	70.32	19.68
K_2	9.56 10-3	36000	90.00	0
	9.77 10-3	34552	86.38	3.62
	10.2 10-3	31751	79.37	10.63
	10.55 10-3	29718	74.29	15.71
	10.7 10-3	28908	72.27	17.73
	10.85 10-3	28130	70.32	19.68

The total capacity loss presents the sum of the loss due to corrosion of the electrodes, stratification of the electrolyte, hard sulfating of the electrodes and poor-cohesion of the active mass. This total rated capacity loss is given by the following equation:

$$\Delta C = \Delta C_{corrosion} + \Delta C_{sulfating} + \Delta C_{Poor-cohesion} \quad (6)$$

With

$\Delta C_{corrosion}$ is the rated battery capacity loss due to the electrode corrosion and the electrolyte stratification.

$\Delta C_{sulfating}$ is the rated battery capacity loss due to the sulfating phenomena

$\Delta C_{Poor\text{-}cohesion}$ is the rated battery capacity loss due to the poor-cohesion of the active mass.

From equation (6) and (7), the available rated capacity is determined by the following equation:

$$C_{arc} = C_{man} - (\Delta C_{corrosion} + \Delta C_{sulfating} + \Delta C_{Poor-cohesion}) \quad (7)$$

In this context, the analysis of the impact of the parameter variation on the available rated capacity is done. Figure 6 presents the various rated capacity loss as a function of the associated parameters. For these different curves, the main goal is to develop mathematical functions that have the best fit to a series of data points. In fact, the rated capacity loss related to the each degradation mode is estimated using linear approximations.

The $\Delta C_{corrosion}$ is related to the variation of R_{Ω}, the $\Delta C_{Poor\text{-}cohesion}$ is related to the variation of R_{tc} while the $\Delta C_{sulfating}$ is estimated as a function of K_1 and K_2. For that, an estimated polynomial expression of the various capacity loss as a function of each electrical parameter is done by equation (8)- (10).

$$\Delta C_{corrosion} = \sum_{i=0}^{n} a_i * R_{\Omega}^{i} \quad (8)$$

$$\Delta C_{Poor-cohesion} = \sum_{i=0}^{n} b_i * R_{tc}^{i} \quad (9)$$

$$\Delta C_{sulfating} = \Delta C_{sulfating1} + \Delta C_{sulfating2} = \sum_{i=0}^{n} c_i * K_1^{i} + \sum_{i=0}^{n} d_i * K_2^{i} \quad (10)$$

The curves-fitting by Ordinary Least Square procedure (OLS) allows to obtain the polynomial expressions that adequately describes the rated capacity loss of the battery related to the each degradation mode. The approximation results show that:

The $\Delta C_{corrosion}$ expression is given by equation (11).

$$\Delta C_{corrosion} = 443 * R_{\Omega} - 10.72 \quad (11)$$

The $\Delta C_{Poor\text{-}cohesion}$ expression can be obtained by equation (12).

$$\Delta C_{Poor-cohesion} = 443.3 * R_{tc} - 16.05 \quad (12)$$

The $\Delta C_{sulfating1}$ expression is given as a function of K_1 by equation (13).

$$\Delta C_{sulfating1} = -0.136 * K_1 + 87.75 \quad (13)$$

Equation (14) can be used to describe the $\Delta C_{sulfating2}$ expression as a function of K_2.

$$\Delta C_{sulfating2} = -1.866 * 10^6 * K_2^2 + 5.343 * 10^4 * K_2 - 340.3 \quad (14)$$

Finally, the available rated capacity expression is the following.

$$C_{arc} = C_{man} - (443 * R_{\Omega} + 443.3 * R_{tc} - 0.136 * K_1 - 1.866 * 10^6 * K_2^2 + 5.343 * 10^4 * K_2 - 279.32) \quad (15)$$

4. Lifetime battery estimation

The estimation of the battery ageing is based on the creation of several indicators in order to quantify its lifetime. The main used indicator in the literature is the number of remaining cycles ($N_{remaining\text{-}cycle}$). In this context, a diagnostic system that allows the calculation of $N_{remaining\text{-}cycle}$ related to the depth of discharge is developed to estimate the battery lifetime.

4.1. Diagnostic system

In the standalone photovoltaic applications, the battery lifetime is typically controlled by the gradual decreasing of its available capacity. Consequently, the most critical lifetime indicator is the number of remaining cycles of the used battery. A lead acid battery is declared defective if it shows a capacity loss ΔC at fully charge equal 20% of its rated capacity C_{man} which is the industry standard end of life definition [34]. In this context, the rated capacity loss is generally stands in relationships to the number of remaining cycles. The variation of ΔC as a function of the number of remaining cycles $N_{remaining\text{-}cycle}$ is linear (Figure 7).

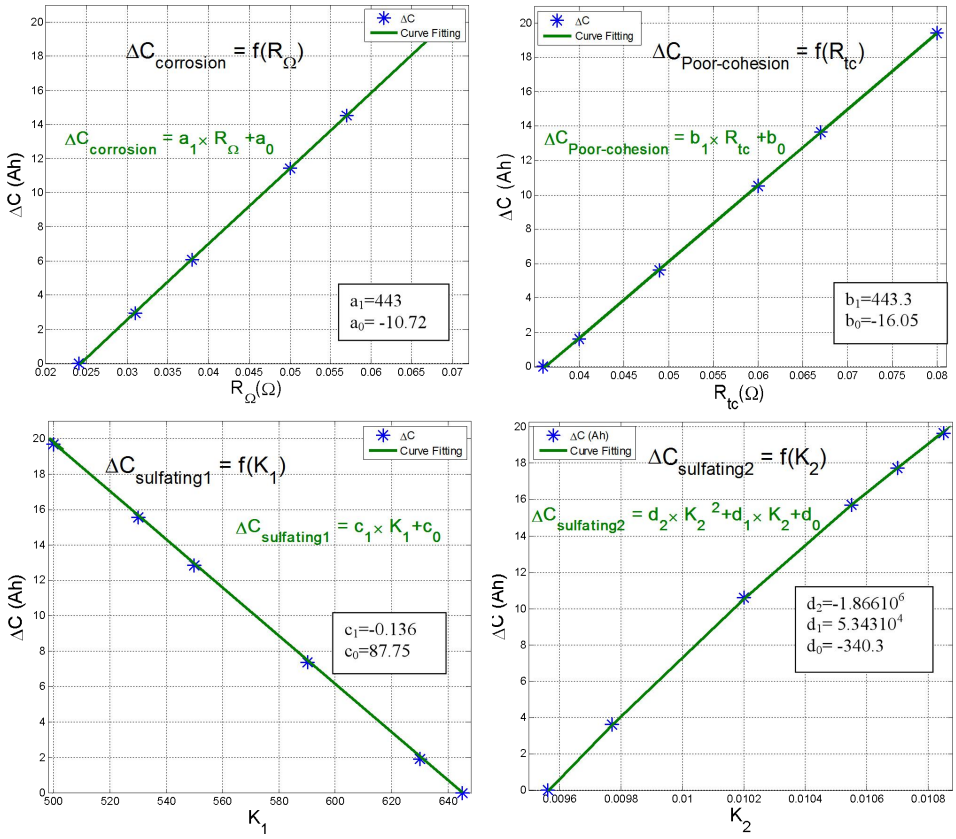

Fig. 6. Capacity loss related to each degradationsmode as a function of the parameters variation.

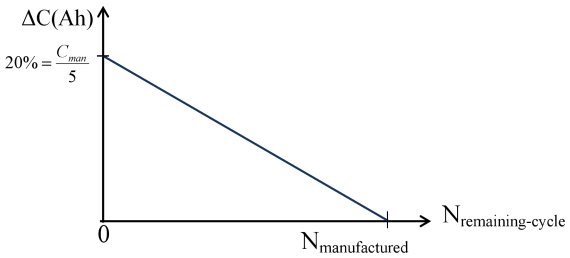

Fig. 7. Rated battery capacity loss as a function of the number of remaining cycles

For that, the battery capacity loss can be defined as:

$$\Delta C = \frac{C_{man}}{5} * (1 - \frac{N_{remaining-cycle}}{N_{manufactured}}) \quad (16)$$

With$N_{manufactured}$ is the number of manufactured cycles given by the manufacturer.
The number of remaining cycle's expression is given by:

$$N_{remaining-cycle} = \left(1 - \frac{5\Delta C}{C_{man}}\right) * N_{manufactured} \quad (17)$$

The choice of the Depth Of Discharge (DOD) limit is a key parameter in the analysis and estimation of the lead acid battery performances. Therefore, the authors propose to integrate the effect of the depth of discharge in the mathematical aging model. Battery manufacturers generally characterizes the lifetime in terms of a maximum number of manufactured cycles $N_{manufactured}$ for different DOD [35]. For that, it usually provides the experiment datasheet to describe their relationship. Figure 8 presents the evolution of the number of manufactured cycles as a function of DOD for lead acid battery using experimental data.

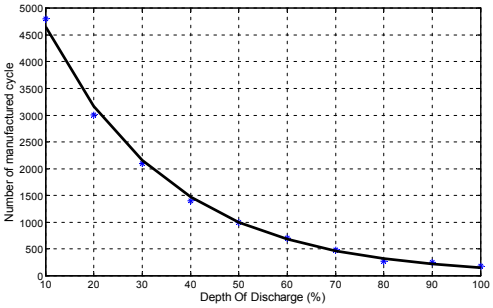

Fig. 8. Number of battery manufactured cycles as a function of DOD (manufacturer's data)

The result shows that the influence of DOD has an exponential form on the number of manufactured cycles $N_{manufactured}$. In this context, the $N_{manufactured}$ is estimated by using the exponential function as shown in equation (18).

$$N_{manufactured} = 6837 * e^{-0.038*DOD} \quad (18)$$

The basic relationship between the number of remaining cycles, the depth of discharge and capacity loss is determined by the following equation:

$$N_{remaining-cycle} = \left(1 - \frac{5\Delta C}{C_{man}}\right) * 6837 * e^{-0.038*DOD} \quad (19)$$

The diagnostic system also includes an analysis of the produced global capacity of the battery during its lifecycle. This global capacity presents the total amount of energy during its operating where its evolution depends most strongly on the interrelationship between DOD and $N_{manufactured}$. Equation (20) gives the formula for calculating the global capacity of a new battery ($GC_{New\text{-}battery}$).

$$GC_{New-battery} = N_{manufactured} * \frac{C_{man}*DOD}{100} \quad (20)$$

Figure 9 shows the evolution of the global capacity of a new battery as a function of DOD. The results show that the optimum choice of the DOD is 26%.

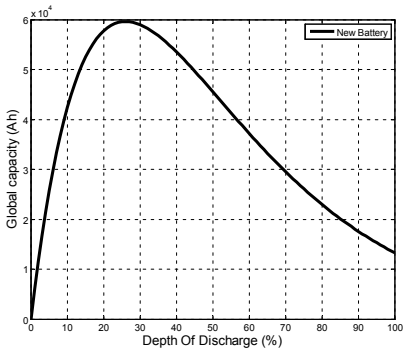

Fig. 9. Global capacity of a new battery as a function of DOD

The global capacity of used battery has the following mathematical expression (21).

$$GC_{used-battery} = N_{remaining-cycle} * \frac{C_{arc} * DOD}{100}$$

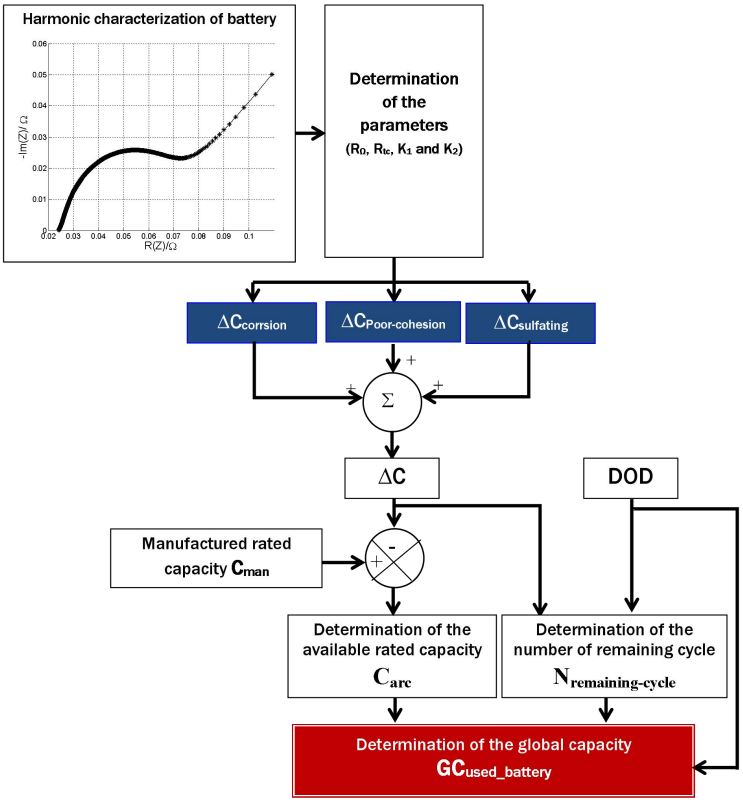

Fig. 10.Diagnostic system for estimating the battery lifetime

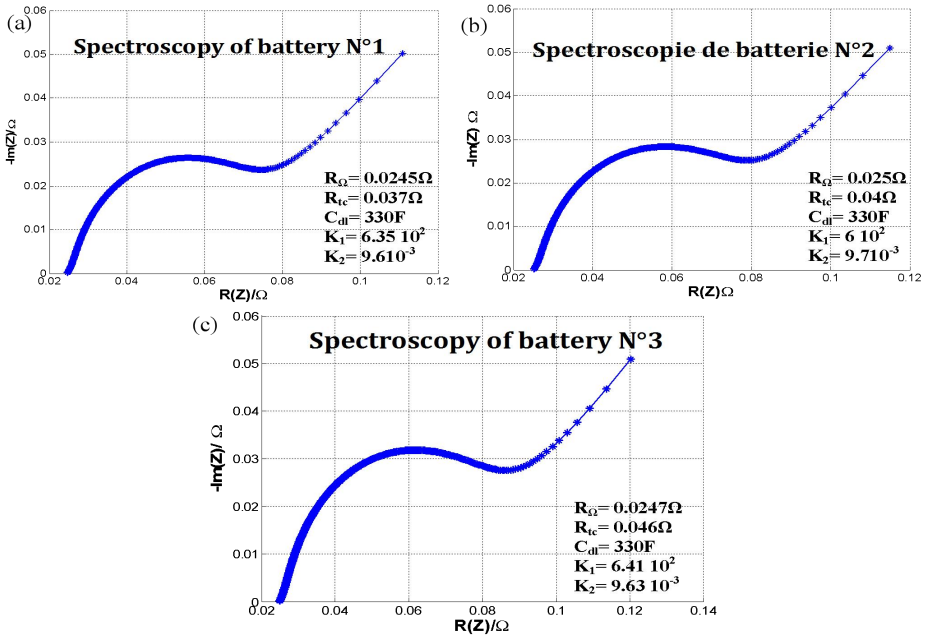

Fig. 11.Responses voltage of: a) the first battery; b) the second battery

A recapitulation of available rated capacity for each battery is shown in Table 3.

Table 3: Aging rate of each battery

	Battery N°1	Battery N°2	Battery N°3
$\Delta c_{corrosion}$ (Ah)	0.1335	0.355	0.222
$\Delta c_{Poor-\ cohesion}$ (Ah)	0.3521	1.682	4.341
$\Delta c_{sulfating}$ (Ah)	2.047	8.549	1.757
Available rated capacity C_{arc}(Ah)	87.468	79.414	83.678
Rated capacity loss ΔC (Ah)	2.532	10.586	6.320

Battery N°1 (Fig.11 (a)) has a rated capacity loss equal to 2.532Ah due to the appearance of the electrode corrosion, hard sulfating phenomena and the poor-cohesion of the active mass. Indeed, the variation of the interne resistance R_Ω generates the rated capacity loss by the electrode corrosion in order of 0.1335Ah.The variation of R_{tc} shows a rated capacity loss in order of 0.3521Ah associated to the poor-cohesion of the active mass. The sulfating phenomenon represents by the variation of Z_ω which generates a capacity loss of 2.047Ah.

The rated capacity loss of the battery N°2 (Fig.11 (b)) is equal to 10.586. This rated capacity loss is due to the poor-cohesion of active mass in order of 1.682Ah and the hard sulfating phenomenon in order of 8.549Ah. The battery N°3 (Fig.11 (c)) has a rated capacity loss equal to 6.320Ah that presents the sum of the electrode corrosion loss in order of 0.222Ah, hard sulfating phenomena loss in order of 1.757Ah and the poor-cohesion of the active mass loss in order of 4.341Ah.

The calculation of the capacitance losses of the tested batteries allows estimating the number of remaining cycles according to DOD. Equation (19) allows plotting the curve of the evolution of $N_{remaining-cycle}$ as a function of DOD for three batteries as illustrated in Figure 12.

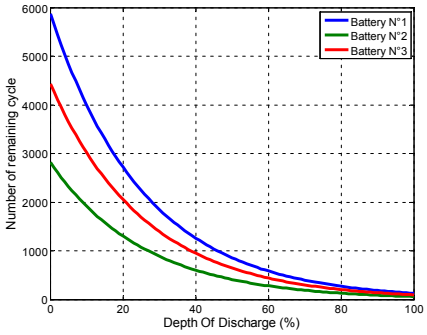

Fig. 12. Number of remaining cycles as a function of DOD

For the increase of DOD every 10% until reach the value 100%, the respective $N_{remaining-cycle}$ of the three used batteries are grouped in the Table 4.

Table 4: Available rated capacity of each battery

DOD (%)	$N_{remaining-cycle}$		
	Battery N°1	Battery N°2	Battery N°3
10	4000	1916	3019
20	2720	1300	2054
30	1851	887	1398
40	1260	604	951
50	857	411	647
60	583	280	441
70	397	190	300
80	270	129	240
90	183	88	139
100	125	60	94

Usually in the standalone PV application, the maximum DOD is fixed at 50% in order to avoid the deep discharge which causes the electrolyte stratification and the hard sulfating of the electrode [4,9]. In this case, the number of remaining cycles is respectively 857 for the battery N°1with global capacity equal to 37480Ah and 411 for the battery N°2with global capacity equal to 16320 Ah. The battery N°3 has a number of remaining cycles equal to 647 with global capacity equal to 27086Ah.For battery aging, it is necessary to represent the evolution of the global capacity as a function of the depth of discharge in order to find the maximum lifetime by an optimal choice of DOD. Figure 13 shows the global capacity of the batteries as a function of DOD.

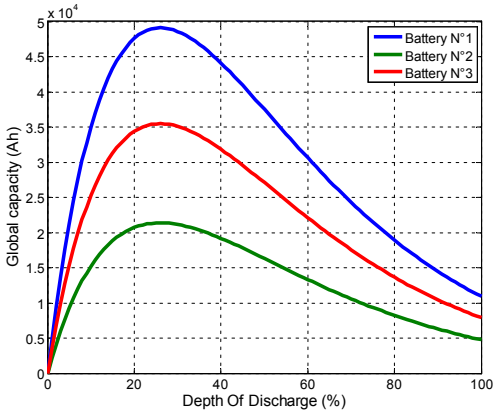

Fig. 13.Global capacity of the three batteries as a function of DOD

The results show that when DOD is 26%, the$GC_{used\text{-}battery}$is 49115Ah for battery N°1, 21381Ah for batteryN°2 and 35477Ah for battery N°3. Consequently, this paper provides an accurate approach for estimating battery lifetime. Particularly, the influence of DOD is considered in this new methodology. However, the proposed mathematical aging model allows predicting the number of remaining cycles precisely at different DOD. For that, a suitable choice of DOD is request to improve the battery use efficiency.

5. Conclusion

The overall scope of this research work was to develop a new methodology lifetime estimation using the voltage drops to determinate the number of remaining cycles of the battery. This method allows predicting the exploitation period of the storage system under optimum conditions related to the depth of discharge. In fact, the complete methodology for the available capacity analysis was presented. It is based on the study of the correlation between the various electrical equivalent circuit parameters and the degradation modes (stratification of electrolyte, corrosion of electrodes, hard sulfating of electrodes and poor-cohesion of active mass). Then, a mathematical expression is developed to describe adequately the available rated capacity as a function of electrical equivalent circuit parameters.

After that, a diagnostic system is developed to estimate the battery lifetime by the calculation of the number cycle remaining as a function of the depth of discharge. The validation of this diagnostic system is assured by an analysis of the experimental discharge characteristic of three lead-acid batteries. The determination of the different electrical parameters of the used batteries allows to calculate the available rated capacity and to estimate the number of remaining cycles which taken into account the depth of discharge. From these data, the battery global capacity is calculated so that is possible to choice of optimal DOD. The results show that a choice of DOD of 26% presents a higher global capacity and ensure the maximum battery lifetime. Finally, the aims of developing reliable, realistic and scalable methodology lifetime estimation for battery storage in the standalone photovoltaic applications were successfully achieved.

References

[1] A. Jossen, J. Garche D. Uwe Sauer. "Operation conditions of batteries in PV applications". Solar Energy 2004, 76, 759–769.

[2] S. Schaeck, A.O. Stoermer, E. Hockgeiger. "Micro-hybrid electric vehicle application of valve-regulated lead–acid batteries in absorbent glass mat technology: Testing a partial-state-of-charge operation strategy". Journal of Power Sources 2009; 190:173-183.

[3] R. Yahmadi, K.Brik, F. Ben Ammar, "Sizing and improving performances of a photovoltaic water pumping system for irrigation in Jerid Tunisia" 2019 10th International Renewable Energy Congress (IREC), Sousse, Tunisia, 2019, pp. 1-6, doi: 10.1109/IREC.2019.8754534.

[4] I. Azzouz, I. Hammami, K.Brik, F. Ben Ammar, "Integration of multi-criteria decision-making for performance evaluation of different solar batteries technologies"Electrical Engineering, Volume 105, Issue 2, Pages 775 - 795April 2023.

[5] K. Brik, F. Ben Ammar, "Improved performance and energy management strategy for proton exchange membrane fuel cell/backup battery in power electronic systems". Int J Hydrogen Energy 2017; 42:8845-8856.

[6] L.Gaines. The future of automotive lithium-ion battery recycling: Charting a sustainable course. Sustainable Materials and Technologies 2014;1: 2-7.

[7] J. Schiffer, D. Uwe Sauer, H. Bindner, Tom Cronin, Per Lundsager, Rudi Kaiser. "Model prediction for ranking lead-acid batteries according to expected lifetime in renewable energy systems and autonomous power-supply systems". J of Power Sources 2007;168: 66-78.

[8] H. Wenzl, I. Baring-Gould, R. Kaiser, B. Yann Liaw, P. Lundsager, J. Manwell, A. Ruddell, V. Svoboda, "Life prediction of batteries for selecting the technically most suitable and cost effective battery". Journal of Power Sources2005;144:373–384.

[9] R. Dufo-López, J. M. Lujano-Rojas, L. Bernal-Agustín . "Comparison of different lead–acid battery lifetime prediction models for use in simulation of stand-alone photovoltaic systems". Applied Energy 2014;115: 242253.

[10] D. Gallo, Carmine Landi, Mario Luiso and Rosario Morello. "Optimization of Experimental Model Parameter Identification for Energy Storage Systems". Energies 2013; 6:4572–4590.

[11] I. Azzouz, R. Yahmadi, K. Brik, et al. Analysis of the critical failure modes and developing an aging assessment methodology for lithium iron phosphate batteries. Electrical Engineering, Volume 104, 27–43 (2022). doi.org/10.1007/s00202-021-01320-7.

[12] T.M.Layadi, G.Champenois, M.Mostefai, D.Abbes."Lifetime estimation tool of lead–acid batteries for hybrid power sources design. Simulation Modelling Practice and Theory 2015;54:36-48.

[13] C.in, A.Tang ,W.Wang. "A review of SOH estimation methods in Lithium-ion batteries for electric vehicle applications". Energy Procedia 2015;75:19201925.

[14] B.Y. Liaw, R.G. Jungst, G. Nagasubramanian, H.L. Case, D.H. Doughty. "Modeling capacity fade in lithium-ion cells". J Power Sources, 2005;140: 157-161.

[15] V. Ramadesigan, K. Chen, N.A. Burns, V. Boovaragavan, R.D. Braatz, V.R. Subramanian, Parameter estimation and capacity fade analysis of lithium-ion batteries using reformulated models. Journal of the Electrochemical Society 2011; 158 : 1048–1054.

[16] M. Safari, C. Delacourt. Mathematical modeling of lithium iron phosphate electrode: Galvanostatic charge/discharge and path dependence. Journal of the Electrochemical Society 2011;158: 62–73.

[17] I. Gonzlez, A. Ramiro, M. Calderon, A.J. Calderon, J.F. Gonzlez. "Estimation of the state-of-charge of gel lead-acid batteries and application to the control of a stand-alone wind-solar test-bed with hydrogen support. International Journal of Hydrogen Energy 2012:37; 11090-11103.

[18] J. Wang, P. Liu, J. Hicks-Garner, E. Sherman, S. Soukiazian, M. Verbrugge, H. Tataria, J. Musser, P. Finamore. Cycle-life model forgraphite-LiFePO 4 cells.J. Power Sources 2011; 196:3942–3948

[19] M. Ceraolo.New dynamical models of lead-acid batteries. IEEE Trans. Power Syst 2000; 15: 1184–1190.

[20] B.Y. Liaw, R.G. Jungst, G. Nagasubramanian, H.L. Case, D.H. Doughty. " Modeling capacity fade in lithium-ion cells". Journal of Power Sources 2005;140: 157–161.

[21] M. Ecker, J.B. Gerschler, J. Vogel, S. Kbitz, F. Hust, P. Dechent, D.U. Sauer. Development of a lifetime prediction model for lithium-ionbatteries based on extended accelerated aging test data. J Power Sources 2012; 215 :248–257.

[22] J. Kozlowski, Electrochemical Cell Prognostics Using Online Impedance Measurements and Model-based Data Fusion Techniques, in: IEEEAerospace Conference 2003;7:3257–3270.

[23] Y.Zou, H.Xiaosong,M.Hongmin, L.Shengbo. CausalCombined State of Charge and State of Health estimation over lithium-ion battery cellcycle lifespan for electric vehicles. Journal of Power Sources 2015;273:793–803.

[24] C.Fleischer, W. Waag, H.Heyn, D.Sauer. On-line adaptive battery impedance parameter and state estimation considering physical principlesin reduced order equivalent circuit battery models, Part 1. Requirements, critical review of methods and modeling. Journal of Power Sources2014;260:276–291.

[25] K. Benabdelaziz. M. Maaroufi. Battery dynamic energy model for use in electric vehicle simulation. International Journal of HydrogenEnergy 2017: 42; 19496-19503.

[26] K. Brik, F. Ben Ammar. Causal tree analysis of depth degradation of the lead acid battery. J.Power Sources 2013;228:39-46.

[27] B. Bogno, J. Sawicki, T. Salame, M. Allierie, F.Sanit-Eve, O.Hamandjoda, B.Tibi. Improvement of safety, longevity and performance of leadacid battery in off-grid PV systems. International Journal of Hydrogen Energy 2017: 42;3466-3478.

[28] A. Mohammedi, D. Rekioua , T. Rekioua, S. Bacha. Valve Regulated Lead Acid battery behavior in a renewable energy system under an ideal Mediterranean climate. International Journal of Hydrogen Energy 2016: 41; 20928-20938.

[29] K. Brik, F. Ben Ammar. The fault tree analysis of the lead acid battery degradation. J of electrical systems 2008;4-2:1–12.

[30] D.U.Sauer, H,Wenzl. Comparison of different approaches for lifetime prediction of electrochemical systemsUsing lead-acid batteries as example . Journal of Power Sources 2008; 176: 534–546

[31] A.Barr, B.Deguilhem, S. Grolleau, M.Grard,F.Suard, D.Riu. A review on lithium-ion battery ageing mechanisms and estimations for automotive applications . Journal of Power Sources 2013;241:680–689.

[32] D.A.J. Rand, D.P. Boden, C.S. Lakshmi, R.F. Nelson, R.D. Prengaman.Manufacturing and operational issues with lead-acid batteries.Journal of Power Sources 2002; 107: 280–300.

[33] P.Detchko. Chapter 3 H2SO4 ElectrolyteAn Active Material in the LeadAcid Cell. Lead-Acid Batteries: Science and Technology (Second Edition)2017; 133–167.

[34] E.Krieger, J.Cannarella,C.Arnold. A comparison of lead-acid and lithium based battery behavior and capacity fade in o -grid renewable charging applications. Energy 2013;60:492–500.

[35] M.Behzadi, M.Niasati. Comparative performance analysis of a hybrid PV/FC/battery stand-alone system using di erent power management strategies and sizing approaches . International journal of hydrogen energy 2015;4:538–548.